offer the possibility to study bicentric metal-centered reactions between chiral complexes and chiral or prochiral substrates in order to achieve asymmetric syntheses.

Formation of $[Fe_2(CO)(NO)(\mu\text{-}"S_4")_2]PF_6$ (**3**) from **2** and $NOPF_6$ proves the accessibility of coordination sites at the iron centers in **2**. Surprisingly, only one of the two CO ligands in **2** can be substituted by NO^+. This indicates an interaction of the iron centers via thiolato bridges such that the CO/NO^+ substitution at one iron center reduces the electron density at the second iron center in the molecule, preventing the substitution of the second CO ligand. Interaction between the iron centers is also revealed by IR and Mössbauer spectra of **2** and **3**.

The iron centers of **2** are 18-electron configurated. Substitution of the 2-electron donor CO by the 3-electron donor NO leads to metal centers exceeding the noble gas configuration. As a consequence, the Fe–S(thiolato) bridges are cleaved, and mononuclear 18-electron configurated $[Fe(NO)_2("S_4")]$ (**4**) forms in which the "S_4" ligand acts as tridentate ligand only. Drastic conditions are required for the reactions of **2** with PMe_3 and MeLi, respectively. They lead also to cleavage of **2** into mononuclear entities and formation of $[Fe(CO)(PMe_3)("S_4")]$ (**5**) in the case of PMe_3. With MeLi, the final reaction product is the binuclear anion $[Fe("S_2")_2]_2^{2-}$ (**6**). The results show that mononuclear iron carbonyl complexes with multidentate thioether thiolato ligands can be used as synthons for the synthesis of binuclear and possibly even polynuclear complexes. The binuclear complexes described here have model character for several iron oxidoreductases with respect to their structure, e.g., coordination sphere of sulfur and chirotopicity of metal centers, as well as to their reactivity shown by the coordination of "soft" σ–π ligands CO and NO to the iron centers.

Acknowledgment. These investigations were supported by the Deutsche Forschungsgemeinschaft and by the Fonds der Chemischen Industrie. We gratefully acknowledge this support.

Supplementary Material Available: Listings of crystallographic data and data collection procedures, anisotropic thermal parameters, complete bond distances and bond angles, and fractional coordinates of atoms and isotropic thermal parameters (15 pages); listings of F_o and F_c values (24 pages). Ordering information is given on any current masthead page. Further details of the X-ray crystal structure analysis have been deposited with the Fachinformationszentrum Energie, Physik, Mathematik, D-7514 Eggenstein-Leopoldshafen 2, FRG, and can be obtained by quoting the deposition number (CSD-320152 (**2**), CSD-320153 (**1**)), the authors' names, and the reference.

Contribution from the Laboratoire de Chimie de Coordination du CNRS,† 205 route de Narbonne, 31077 Toulouse Cedex, France, and National Research Center "Demokritos", 15310 Aghia Paraskevi, Athens, Greece

Iron(II) Complexes of 2,2′-Biimidazole and 2,2′-Bibenzimidazole as Models of the Photosynthetic Mononuclear Non-Heme Ferrous Sites. Synthesis, Molecular and Crystal Structure, and Mössbauer and Magnetic Studies

Didier Boinnard,[1a] Patrick Cassoux,[1a] Vasili Petrouleas,[1b] Jean-Michel Savariault,[1a] and Jean-Pierre Tuchagues*,[1a]

Received January 22, 1990

A series of seven high-spin ferrous complexes of 2,2′-biimidazole and 2,2′-bibenzimidazole ligands have been prepared and studied with IR and Mössbauer spectroscopy and variable-temperature magnetic susceptibility. The crystal and molecular structures of $[Fe(bbzimH_2)_3](ClO_4)_2 \cdot H_2O$ (**1**) and $[Fe(bbzimH_2)_3]Cl_2 \cdot MeOH \cdot 4.33H_2O$ (**2**) have been determined. **1** crystallizes in the monoclinic system, space group $P2_1/c$, with $Z = 4$ and $a = 13.564$ (3) Å, $b = 19.122$ (3) Å, $c = 18.328$ (5) Å, and $\beta = 109.82$ (2)°. **2** crystallizes in the hexagonal system, space group $R\bar{3}$, with $Z = 6$ and $a = 15.509$ (3) Å and $c = 37.989$ (7) Å. The structure of **1** consists of the mononuclear cations $[Fe(bbzimH_2)_3]^{2+}$ separated by ClO_4^- anions and molecules of water of crystallization. The structure of **2** includes $[Fe(bbzimH_2)_3]^{2+}$ cations with two chloride anions and one water molecule statistically disordered over three sites. Steric hindrance considerations indicate that the $bbzimH_2$ ligands of $Fe(bbzimH_2)_2Cl_2$ (**4**) and $Fe(bbzimH_2)_2](HCO_2)_2$ (**7**) are cis to each other as confirmed by the Mössbauer spectroscopy results. A trans arrangement of the $bimH_2$ ligands of $Fe(bimH_2)_2Cl_2$ (**3**) and $Fe(bimH_2)_2(HCO_2)_2$ (**6**), although implying some steric hindrance, is favored by the Mössbauer results. The Mössbauer spectroscopy and variable-temperature magnetic susceptibility results obtained provide evidence that the seven complexes described herein are mononuclear high-spin iron(II) species experiencing zero-field splitting of the iron(II) ground state. The distortion of the coordination sphere is predominantly axial for **2**–**4**, **6** and **7** and rhombic for **1** and **5** ($Fe(bimH_2)_2(CH_3CO_2)_2$). Complex **5** shows two iron(II) sites possibly corresponding to a mixture of cis and trans arrangements. This complex shows the closest similarity to the bacterial reaction centers and photosystem 2 ferrous sites. The large variability in the Mössbauer properties in this rather similar set of complexes indicates that in addition to the nature of the ligands the distortion of the Fe(II) coordination sphere is a factor that has to be taken into account in designing proper spectral analogues of the photosynthetic iron(II) complex.

Introduction

The reaction centers of photosynthetic bacteria[2] and the photosystem 2 of oxygenic photosynthetic organisms[3] have been shown to include a ferrous ion between the primary and the secondary quinone electron acceptors. The X-ray molecular structure determination of the reaction center of *Rhodopseudomonas viridis*[4] and *R. sphaeroides*[5] indicates that the ferrous ion is in a distorted-octahedral ligand environment including four nitrogen atoms pertaining to the imidazole moiety of histidine residues and two oxygen atoms from a glutamic acid residue of the surrounding protein. A similar iron coordination has been evidenced for native soybean lipoxygenase-1.[6] This enzyme pertains to the family of mononuclear non-heme-iron-containing dioxygenases that catalyze

† Unité No. 8241 liée par Conventions à l'Université Paul Sabatier et à l'Institut National Polytechnique de Toulouse.

(1) (a) Laboratoire de Chimie de Coordination du CNRS. (b) National Research Center "Demokritos".
(2) Clayton, R. K., Sistrom, W. R., Eds. *The Photosynthetic Bacteria*; Plenum: New York, 1978.
(3) (a) Nugent, J. H. A.; Diner, B. A.; Evans, M. C. W. *FEBS Lett.* **1981**, *124*, 241–244. (b) Petrouleas, V.; Diner, B. A. *FEBS Lett.* **1982**, *147*, 111–114. (c) Petrouleas, V.; Diner, B. A. *Adv. Photosynth. Res., Proc. Int. Congr. Photosynth. 6th* **1984**, *1*, part 2, 195–198. (d) Rutherford, A. W.; Zimmerman, J. L. *Biochim. Biophys. Acta* **1984**, *767*, 168–175. (e) Diner, B. A.; Petrouleas, V. *Ibid.* **1986**, *849*, 264–275.
(4) (a) Deisenhofer, J.; Epp, O.; Miki, K.; Huber, R.; Michel, H. *J. Mol. Biol.* **1984**, *180*, 385–398. (b) Deisenhofer, J.; Epp, O.; Miki, K.; Huber, R.; Michel, H. *Nature* **1985**, *318*, 19–26. (c) Michel, H.; Epp, O.; Deisenhofer, J. *EMBO J.* **1986**, *5*, 2445–2451.

0020-1669/90/1329-4114$02.50/0 © 1990 American Chemical Society

a variety of reactions including oxygenation of benzene and benzoic acid to dihydrocatechols, oxygenation of catechols, α-keto acid dependent hydroxylation of proline residues in collagen, and peroxidation of unsaturated fatty acids.[7]

Two iron(II) complexes including 2,2'-biimidazole as ligands have been previously synthesized,[8,9] neither of which has been structurally characterized or thoroughly studied. However, the X-ray molecular structure of a ferric complex including two 2,2'-biimidazole ligands has been already described.[10] Owing to the interest of such ferrous complexes as models of the ferrous ion of mononuclear non-heme-iron-containing proteins, we have synthesized and studied several chelates resulting from the reaction of 2,2'-biimidazole ($bimH_2$) and 2,2'-bibenzimidazole ($bbzimH_2$) with ferrous chloride, ferrous perchlorate, ferrous acetate, and ferrous formate. In this paper, we report the synthesis and IR, Mössbauer, and variable-temperature magnetic susceptibility results for $[Fe(bbzimH_2)_3](ClO_4)_2$ (**1**), $[Fe(bbzimH_2)_3]Cl_2$ (**2**), $Fe(bimH_2)_2Cl_2$ (**3**), $Fe(bbzimH_2)_2Cl_2$ (**4**), $Fe(bimH_2)_2(CH_3CO_2)_2$ (**5**), $Fe(bimH_2)_2(HCO_2)_2$ (**6**), and $Fe(bbzimH_2)_2(HCO_2)_2$ (**7**). X-ray crystal structure determinations of **1** and **2** and conformational studies of **3**–**7** based on the X-ray crystal structure determination of parent complexes have also been performed with the aim of giving a detailed interpretation of their Mössbauer and magnetic properties.

Experimental Section

Materials. All chemicals used for the preparation of the ligands and their metal chelates were of analytical grade. Solvents were degassed under vacuum prior to use. Ferrous acetate and ferrous formate were prepared according to the method of Schreurer-Kestner[11] as modified by Rhoda et al.[12]

Ligands. 2,2'-Biimidazole ($bimH_2$) was prepared according to the literature method.[13] 2,2'-Bibenzimidazole ($bbzimH_2$) was prepared according to the method of Lane[14] as modified by Fieselman et al.[13]

Complexes. The ferrous salt ($Fe(ClO_4)_2\cdot 6H_2O$, $FeCl_2\cdot 4H_2O$, $Fe(CH_3CO_2)_2\cdot 2H_2O$, or $Fe(HCO_2)_2\cdot 2H_2O$) (0.001 mol) was dissolved in a minimum amount of oxygen-free methanol (ca. 20 mL) in a Schlenk vessel. The ligand ($bimH_2$ or $bbzimH_2$) (0.003 mol in the case of **1** and **2** or 0.002 mol in the case of **3**–**7**) was suspended in 100 mL of methanol, and the suspension was degassed in a Schlenk assembly. The complexes were prepared by dropwise transfer of the ferrous salt solution onto the ligand suspension stirred under purified nitrogen. The resulting reaction mixture was warmed to 65 °C for ca. 1 h, during which the ligand dissolved and the metal chelate slowly precipitated as a microcrystalline solid. On completion of the reaction, the mixture was allowed to cool to room temperature and was filtered under vacuum. The resulting complexes were washed with cold methanol and dried under vacuum overnight. The complexes were finally transferred and stored in an inert-atmosphere box (Vacuum Atmospheres HE 43.2) equipped with a dry-train (Jahan EVAC 7).

The analytical results for the complexes are in good agreement with the theoretical values for C, H, N, Cl, and Fe.[15]

Single crystals of **1** and **2** suitable for the X-ray study were obtained by slow concentration of their methanolic solution. **1** crystallizes as the $[Fe(bbzimH_2)_3](ClO_4)_2\cdot H_2O$ hydrate in the form of orange parallelepipeds, while the samples of **1** obtained as orange powders do not include any solvent molecule. **2** crystallizes as the $[Fe(bbzimH_2)_3]Cl_2\cdot MeOH\cdot 4.33H_2O$ solvate in the form of red-brown polyhedra, while the samples of **2** obtained as light-brown powders include only three molecules of water per molecule of complex.

Table I. Crystallographic Data for Complexes **1** and **2**

	1	**2**
formula of the asymmetric unit	$C_{42}H_{32}N_{12}O_9Cl_2Fe$	$C_{43}H_{42.66}N_{12}O_{5.33}Cl_2Fe$
fw	975.55	939.98
a, Å	13.564 (3)	15.509 (3)
b, Å	19.122 (3)	
c, Å	18.328 (5)	37.989 (7)
β, deg	109.82 (2)	
V, Å^3	4472 (3)	7913 (6)
space group	$P2_1/c$ (No. 14)	$R\bar{3}$ (No. 148)
Z	4	6
d_{calcd}, g cm^{-3}	1.45	1.18
t, K	295	295
λ(Mo Kα, graphite monochromator), Å	0.71069	0.71069
μ(Mo Kα), cm^{-1}	5.22	3.95
$R = \sum\|k\|F_o\| - \|F_c\|\|/\sum k\|F_o\|$	0.071	0.100
$R_w = [\sum w(k\|F_o\| - \|F_c\|)^2/\sum wk^2F_o^2]^{1/2}$	0.099	0.152

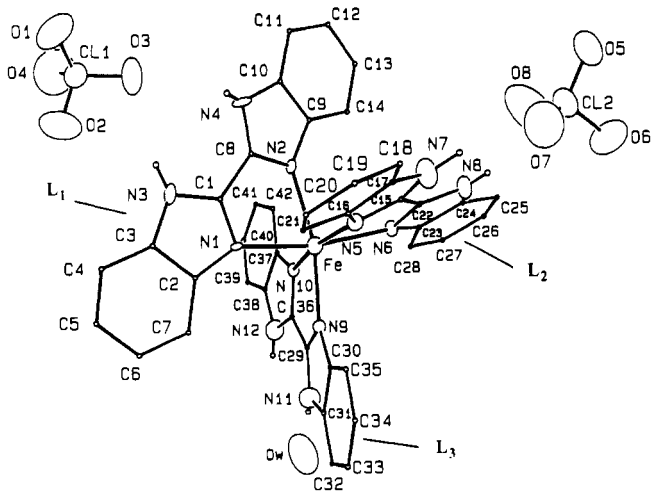

Figure 1. ORTEP view of the $[Fe(bbzimH_2)_3](ClO_4)_2\cdot H_2O$ (**1**) molecule.

Physical Measurements. Elemental analyses were carried out at the Laboratoire de Chimie de Coordination Microanalytical Laboratory in Toulouse for C, H, and N and at the Service Central de Microanalyses du CNRS in Vernaison for Cl and Fe.

IR spectra were recorded on a Perkin-Elmer 983 spectrophotometer coupled with a Perkin-Elmer infrared data station. Samples were run as CsBr pellets prepared under nitrogen in the drybox.

Variable-temperature magnetic susceptibility data were obtained as previously described[16] on polycrystalline and Vaseline paste samples (prepared in the drybox) with a Faraday-type magnetometer equipped with a continuous-flow Oxford Instruments cryostat.

Mössbauer measurements were obtained with a constant-acceleration conventional spectrometer and a $^{57}Co(Rh)$ source. Computer simulations were obtained with a least-squares-fitting program assuming independent Lorentzian lines. Isomer shift values throughout the paper are given with respect to metallic iron at room temperature.

X-ray Crystal Structure Determination of 1 and 2. Crystal data and information relevant to data collection and refinement for **1** and **2** are given in Table I and in the supplementary material. In both cases, the intensities of three standard reflections were monitored throughout the data collection. No significant fluctuation was noticed. The usual Lorentz–polarization factors were applied to the net intensities. Numerical absorption corrections were made.[17]

The starting point of the structures was determined by using direct methods.[18,19] The atomic scattering factors used in subsequent least-

(5) (a) Allen, J. P.; Feher, G.; Yeates, T. O.; Komiya, H.; Rees, D. C. *Proc. Natl. Acad. Sci. U.S.A.* **1988**, *85*, 8487–8491. (b) Allen, J. P.; Feher, G.; Yeates, T. O.; Komiya, H.; Rees, D. C. *Proc. Natl. Acad. Sci. U.S.A.* **1987**, *84*, 5730–5734.
(6) Navaratnam, S.; Feiters, M. C.; Al-Hakim, M.; Allen, J. C.; Veldink, G. A.; Vliegenthart, J. F. G. *Biochim. Biophys. Acta* **1988**, *956*, 70–76.
(7) For example: Nelson, M. J. *Biochemistry* **1988**, *27*, 4273–4278.
(8) Holmes, F.; Jones, K. M.; Torrible, E. G. *J. Chem. Soc.* **1961**, 4790–4794.
(9) Abushamleh, A. S.; Goodwin, H. A. *Aust. J. Chem.* **1979**, *32*, 513–518.
(10) Dance, I. G.; Abushamleh, A. S.; Goodwin, H. A. *Inorg. Chim. Acta* **1980**, *43*, 217–221.
(11) Schreurer-Kestner, M. A. *Bull. Soc. Chim. Fr.* **1863**, *5*, 345.
(12) Rhoda, R. N.; Fraioli, A. V. *Inorg. Synth.* **1953**, *4*, 159–161.
(13) Fieselman, B. F.; Hendrickson, D. N.; Stucky, G. *Inorg. Chem.* **1978**, *17*, 2078–2084.
(14) Lane, E. S. *J. Chem. Soc.* **1953**, 2238.
(15) Supplementary material.
(16) Luneau, D.; Savariault, J.-M.; Cassoux, P.; Tuchagues, J.-P. *J. Chem. Soc., Dalton Trans.* **1988**, 1225–1235.
(17) Coppens, P.; Leiserowitz, L.; Rabinovich, D. *Acta Crystallogr., Sect. B: Struct. Crystallogr. Cryst. Chem.* **1965**, *18*, 1035.
(18) Sheldrick, G. M. *SHELX 76. Program for Crystal Structure Determination*; University of Cambridge: Cambridge, England, 1976.
(19) Sheldrick, G. M. In *Crystallographic Computing 3*; Sheldrick, G. M., Krüger, C., Goddard, R., Eds.; Oxford University Press: Oxford, England, 1985; p 175–179.

Table II. Fractional Atomic Coordinates of Non-Hydrogen Atoms for $[Fe(bbzimH_2)_3](ClO_4)_2 \cdot H_2O$ (**1**) with Estimated Standard Deviations in Parentheses

atom	x/a	y/b	z/c	atom	x/a	y/b	z/c
Fe	0.2672 (1)	0.00858 (8)	0.73064 (8)				
			Bibenzimidazole Ligand 1				
N(1)	0.4054 (6)	−0.0196 (4)	0.8315 (5)	C(5)	0.552 (1)	−0.1229 (7)	1.0354 (7)
N(2)	0.3839 (6)	0.0870 (5)	0.7261 (5)	C(6)	0.440 (1)	−0.1334 (6)	1.0032 (7)
C(1)	0.490 (1)	0.0127 (6)	0.8301 (6)	C(7)	0.3859 (9)	−0.1005 (5)	0.9339 (6)
C(8)	0.479 (1)	0.0690 (6)	0.7697 (6)	C(9)	0.3991 (9)	0.1401 (6)	0.6794 (6)
N(3)	0.5794 (7)	−0.0041 (5)	0.8874 (5)	C(10)	0.5071 (9)	0.1504 (7)	0.6991 (7)
N(4)	0.5567 (8)	0.1058 (6)	0.7559 (7)	C(11)	0.546 (1)	0.2026 (8)	0.6631 (8)
C(2)	0.4404 (8)	−0.0594 (6)	0.8975 (6)	C(12)	0.471 (1)	0.2420 (8)	0.6081 (8)
C(3)	0.5508 (9)	−0.0498 (6)	0.9324 (6)	C(13)	0.364 (1)	0.2324 (7)	0.5896 (7)
C(4)	0.606 (1)	−0.0820 (6)	1.0035 (7)	C(14)	0.327 (1)	0.1801 (6)	0.6252 (6)
			Bibenzimidazole Ligand 2				
N(5)	0.3239 (7)	−0.0527 (5)	0.6497 (5)	C(19)	0.534 (1)	−0.1880 (9)	0.609 (1)
N(6)	0.1606 (7)	0.0382 (5)	0.6166 (5)	C(20)	0.537 (1)	−0.1844 (8)	0.686 (1)
C(15)	0.2834 (8)	−0.0313 (6)	0.5783 (7)	C(21)	0.4699 (9)	−0.1401 (6)	0.7063 (8)
C(22)	0.1938 (8)	0.0174 (6)	0.5602 (7)	C(23)	0.0761 (9)	0.0788 (6)	0.5801 (6)
N(7)	0.3253 (8)	−0.0572 (7)	0.5277 (6)	C(24)	0.0597 (8)	0.0830 (6)	0.5002 (7)
N(8)	0.1346 (9)	0.0427 (6)	0.4892 (5)	C(25)	−0.0243 (9)	0.1201 (7)	0.4460 (8)
C(16)	0.3990 (9)	−0.0995 (6)	0.6465 (7)	C(26)	−0.090 (1)	0.1555 (6)	0.4774 (8)
C(17)	0.403 (1)	−0.1024 (7)	0.5727 (8)	C(27)	−0.076 (1)	0.1507 (7)	0.5559 (8)
C(18)	0.471 (1)	−0.1459 (9)	0.5509 (9)	C(28)	0.0053 (9)	0.1136 (6)	0.6074 (8)
			Bibenzimidazole Ligand 3				
N(9)	0.1766 (7)	−0.0693 (5)	0.7611 (5)	C(33)	0.097 (1)	−0.2748 (8)	0.7671 (7)
N(10)	0.1828 (6)	0.0690 (5)	0.7909 (5)	C(34)	0.169 (1)	−0.2607 (7)	0.7307 (7)
C(29)	0.1189 (9)	−0.0448 (6)	0.8002 (7)	C(35)	0.2014 (9)	−0.1935 (6)	0.7255 (7)
C(36)	0.1236 (9)	0.0302 (7)	0.8177 (6)	C(37)	0.1758 (8)	0.1357 (7)	0.8192 (6)
N(11)	0.0611 (9)	−0.0941 (6)	0.8206 (6)	C(38)	0.1137 (8)	0.1350 (7)	0.8664 (7)
N(12)	0.0803 (8)	0.0656 (7)	0.8629 (7)	C(39)	0.096 (1)	0.1928 (8)	0.9038 (8)
C(30)	0.1587 (8)	−0.1405 (6)	0.7570 (5)	C(40)	0.140 (1)	0.2537 (9)	0.8925 (9)
C(31)	0.0855 (9)	−0.1569 (7)	0.7942 (6)	C(41)	0.200 (1)	0.2568 (8)	0.8432 (9)
C(32)	0.054 (1)	−0.2252 (7)	0.8006 (8)	C(42)	0.2194 (9)	0.1984 (6)	0.8058 (7)
			Perchlorate 1				
Cl(1)	0.8338 (2)	0.0926 (2)	0.9548 (2)	O(3)	0.7547 (8)	0.0982 (8)	0.8842 (6)
O(1)	0.9312 (8)	0.0874 (9)	0.9473 (7)	O(4)	0.832 (1)	0.1498 (7)	−0.0004 (9)
O(2)	0.813 (1)	0.0352 (7)	0.9916 (7)				
			Perchlorate 2				
Cl(2)	0.2242 (3)	−0.0085 (2)	0.3131 (2)	O(7)	0.279 (1)	−0.064 (1)	0.354 (1)
O(5)	0.266 (1)	0.0226 (9)	0.2621 (6)	O(8)	0.9043 (8)	0.9272 (7)	0.8831 (6)
O(6)	0.122 (1)	−0.029 (1)	0.2700 (9)				
			Water Molecule				
Ow	0.9043 (8)	0.9272 (7)	0.8831 (6)				

squares refinements were those proposed by Cromer and Waber[20] with anomalous dispersion effects.[21]

Complex 1. The space group is $P2_1/c$. All non-hydrogen atoms were assigned anisotropic thermal parameters. Hydrogen atoms (except those of the water molecule, which could not be located) were refined with an arbitrary isotropic temperature factor $U = 0.09$ Å^2. The hydrogen atoms of the phenyl rings were included in the calculations with idealized positions (C–H = 0.97 Å). The oxygen atoms O(7) and O(8) exhibit large thermal parameters, indicating a partial disorder of the corresponding perchlorate anion or thermal motion of these atoms. However the Hamilton test[22] did not indicate significant improvement in the refinement when each of these atoms was allowed to occupy two positions, each with different estimated occupancy factors. The highest residual peak of the final difference Fourier map (0.56 e Å^{-3}) is located near oxygen atom O(8) of the perchlorate anion and indicates that the model used in the refinement does not fully accommodate the distribution of the electronic density. This is reflected in the rather high final agreement factor values obtained (Table I).

Positional parameters and bond lengths and angles are listed in Tables II and III, respectively. Atoms are labeled according to Figure 1. Anisotropic temperature factors, hydrogen atom positional parameters, and observed and calculated structure factor amplitudes are given in the supplementary material.

Complex 2. The parameters optimized by the diffractometer correspond to a rhombohedral unit cell, and the data collection was carried out by using this unit cell. A subsequent conversion of the rhombohedral indices to hexagonal ones was made.

A study of the systematic extinctions and of the intensities allowed the selection of the $R3$ and $R\bar{3}$ space groups. Least-squares refinements were conducted in the centrosymmetric space group $R\bar{3}$ on the basis of convincing intensity statistics.[23] Atomic coordinates of the iron and non-hydrogen atoms of the ligands were refined anisotropically. The hydrogen atoms of the phenyl rings were included in the calculations with idealized positions (C–H = 0.97 Å) and refined with an arbitrary isotropic temperature factor $U = 0.09$ Å^2. Both chloride anions are statistically disordered over three equivalent positions with a 0.66 occupancy factor. One molecule of methanol and 4.33 molecules of water per complex were also located. However, as for the chloride anions, there is a statistical disorder of these solvent molecules over three equivalent positions. Consequently, the chloride anions and oxygen and carbon atoms of the methanol and water molecules were refined isotropically. The hydrogen atoms of the water and methanol molecules were neither located nor included in the calculations. The final difference Fourier map did not reveal any important residual electron density, the largest peak, situated near Ow(4), being less than 0.75 e Å^{-3}.

The quite large final agreement factor values obtained (Table I) result probably from the statistical disorder of the chloride anions and water and methanol molecules. Positional parameters and bond lengths and angles are listed in Tables IV and V, respectively. Atoms are labeled

(20) Cromer, D. T.; Waber, J. T. *International Tables for X-ray Crystallography*; Kynoch Press: Birmingham, England, 1974; Vol. IV, Table 2.2.B, pp 99,101.
(21) Cromer, D. T. Reference 20, Table 2.3.1., p 149.
(22) Hamilton, W. C. *Acta Crystallogr., Sect. B: Struct. Crystallogr. Cryst. Chem.* **1965**, *18*, 502–510.
(23) Howells, E. R.; Phillips, D. C.; Rogers, D. *Acta Crystallogr., Sect. B: Struct. Crystallogr. Cryst. Chem.* **1950**, *3*, 210.

Table III. Selected Interatomic Distances (Å) and Bond Angles (deg) for $[Fe(bbzimH_2)_3](ClO_4)_2 \cdot H_2O$ (**1**) with Estimated Standard Deviations in Parentheses

Iron Environment							
Fe–N(1)	2.207 (8)	Fe–N(5)	2.22 (2)	Fe–N(9)	2.12 (2)	Fe–N(10)	2.17 (1)
Fe–N(2)	2.202 (9)	Fe–N(6)	2.175 (8)				
N(1)–Fe–N(2)	77.3 (4)	N(1)–Fe–N(10)	98.6 (3)	N(2)–Fe–N(10)	99.6 (3)	N(6)–Fe–N(9)	100.5 (3)
N(1)–Fe–N(5)	92.4 (3)	N(2)–Fe–N(5)	85.3 (4)	N(5)–Fe–N(6)	76.3 (3)	N(6)–Fe–N(10)	93.3 (3)
N(1)–Fe–N(6)	165.3 (4)	N(2)–Fe–N(6)	92.2 (3)	N(5)–Fe–N(9)	99.8 (4)	N(9)–Fe–N(10)	77.7 (4)
N(1)–Fe–N(9)	90.7 (3)	N(2)–Fe–N(9)	167.2 (4)	N(5)–Fe–N(10)	168.7 (3)		
Bibenzimidazole Ligand 1							
N(1)–C(1)	1.31 (2)	C(8)–N(4)	1.36 (2)	C(2)–C(7)	1.39 (2)	C(9)–C(14)	1.37 (1)
N(1)–C(2)	1.38 (1)	N(3)–H(N3)	0.8 (1)	C(3)–C(4)	1.40 (2)	C(10)–C(11)	1.40 (3)
N(2)–C(8)	1.32 (1)	N(3)–C(3)	1.35 (2)	C(4)–C(5)	1.33 (3)	C(11)–C(12)	1.39 (2)
N(2)–C(9)	1.39 (2)	N(4)–H(N4)	0.7 (1)	C(5)–C(6)	1.44 (3)	C(12)–C(13)	1.38 (2)
C(1)–C(8)	1.52 (2)	N(4)–C(10)	1.34 (2)	C(6)–C(7)	1.38 (1)	C(13)–C(14)	1.38 (2)
C(1)–N(3)	1.34 (1)	C(2)–C(3)	1.43 (1)	C(9)–C(10)	1.40 (2)		
C(1)–N(1)–C(2)	103.6 (8)	C(1)–N(3)–C(3)	105 (1)	C(3)–C(4)–C(5)	118 (1)	N(4–)C(10)–C(9)	109 (1)
C(8)–N(2)–C(9)	105 (1)	C(8)–N(4)–C(10)	105.0 (9)	C(4)–C(5)–C(6)	124 (2)	N(4)–C(10)–C(11)	131 (1)
N(1)–C(1)–C(8)	119 (1)	N(1)–C(2)–C(3)	109 (1)	C(5)–C(6)–C(7)	118 (1)	C(9)–C(10)–C(11)	121 (2)
N(1)–C(1)–N(3)	116 (2)	N(1)–C(2)–C(7)	131 (1)	C(2)–C(7)–C(6)	119 (2)	C(10)–C(11)–C(12)	115 (1)
C(8)–C(1)–N(3)	125 (1)	C(3)–C(2)–C(7)	120.2 (9)	N(2)–C(9)–C(10)	108 (1)	C(11)–C(12)–C(13)	124 (1)
N(2)–C(8)–C(1)	117 (1)	N(3)–C(3)–C(2)	106.6 (9)	N(2)–C(9)–C(14)	129 (1)	C(12)–C(13)–C(14)	121 (1)
N(2)–C(8)–N(4)	115 (1)	N(3)–C(3)–C(4)	133 (2)	C(10)–C(9)–C(14)	123 (1)	C(9)–C(14)–C(13)	117 (1)
C(1)–C(8)–N(4)	128 (2)	C(2)–C(3)–C(4)	120 (1)				
Bibenzimidazole Ligand 2							
N(5)–C(15)	1.31 (1)	C(22)–N(8)	1.37 (1)	C(17)–C(18)	1.39 (2)	C(24)–C(25)	1.42 (1)
N(5)–C(16)	1.38 (2)	N(7)–H(N7)	0.8 (1)	C(18)–C(19)	1.38 (2)	C(25)–C(26)	1.40 (3)
N(6)–C(22)	1.33 (2)	N(7)–C(17)	1.40 (2)	C(19)–C(20)	1.39 (3)	C(26)–C(27)	1.39 (3)
N(6)–C(23)	1.36 (1)	N(8)–C(24)	1.34 (2)	C(20)–C(21)	1.38 (2)	C(27)–C(28)	1.39 (2)
C(15)–C(22)	1.48 (2)	C(16)–C(17)	1.37 (2)	C(23)–C(24)	1.41 (2)		
C(15)–N(7)	1.34 (2)	C(16)–C(21)	1.42 (2)	C(23)–C(28)	1.39 (2)		
C(15)–N(5)–C(16)	103 (2)	C(15)–N(7)–C(17)	104 (2)	C(16)–C(17)–C(18)	124 (1)	C(24)–C(23)–C(28)	118 (1)
C(22)–N(6)–C(23)	104.1 (9)	C(22)–N(8)–C(24)	107 (2)	C(17)–C(18)–C(19)	115 (2)	N(8)–C(24)–C(23)	105.3 (9)
N(5)–C(15)–C(22)	117 (1)	N(5)–C(16)–C(17)	110 (1)	C(18)–C(19)–C(20)	123 (2)	N(8)–C(24)–C(25)	130 (1)
N(5)–C(15)–N(7)	117 (2)	N(5)–C(16)–C(21)	131 (1)	C(19)–C(20)–C(21)	121 (1)	C(23)–C(24)–C(25)	124 (1)
C(22)–C(15)–N(7)	127 (2)	C(17)–C(16)–C(21)	120 (1)	C(16)–C(21)–C(20)	118 (1)	C(24)–C(25)–C(26)	115 (1)
N(6)–C(22)–C(15)	119 (1)	N(7)–C(17)–C16)	106 (1)	N(6)–C(23)–C(24)	111 (2)	C(25)–C(26)–C(27)	121 (1)
N(6)–C(22)–N(8)	114 (2)	N(7)–C(17)–C(18)	130 (1)	N(6)–C(23)–C(28)	132 (2)	C(23)–C(28)–C(27)	119 (1)
C(15)–C(22)–N(8)	128 (1)	C(26)–C(27)–C(28)	123 (1)				
Bibenzimidazole Ligand 3							
N(9)–C(29)	1.31 (2)	C(36)–N(12)	1.35 (2)	C(31)–C(32)	1.40 (2)	C(39)–C(40)	1.35 (2)
N(9)–C(30)	1.39 (1)	N(11)–C(31)	1.38 (2)	C(32)–C(33)	1.36 (2)	C(40)–C(41)	1.41 (3)
N(10)–C(36)	1.30 (2)	N(12)–H(N12)	0.8 (2)	C(33)–C(34)	1.38 (2)	C(41)–C(42)	1.38 (2)
N(10)–C(37)	1.39 (2)	N(12)–C(38)	1.40 (2)	C(34)–C(35)	1.37 (2)		
C(29)–C(36)	1.47 (2)	C(30)–C(31)	1.42 (2)	C(37)–C(38)	1.40 (2)		
C(29)–N(11)	1.36 (2)	C(30)–C(35)	1.39 (2)	C(38)–C(39)	1.36 (2)		
C(29)–N(9)–C(30)	105 (2)	C(29)–N(11)–C(31)	106 (1)	C(31)–C(32)–C(33)	115 (1)	N(12)–C(38)–C(37)	104 (1)
C(36)–N(10)–C(37)	105 (2)	C(36)–N(12)–C(38)	108 (1)	C(32)–C(33)–C(34)	124 (1)	N(12)–C(38)–C(39)	133 (1)
N(9)–C(29)–C(36)	119 (1)	N(9)–C(30)–C(31)	109 (2)	C(33)–C(34)–C(35)	121 (1)	C(37)–C(38)–C(39)	123 (1)
N(9)–C(29)–N(11)	114 (2)	N(9)–C(30)–C(35)	131 (1)	C(30)–C(35)–C(34)	118 (1)	C(38)–C(39)–C(40)	117 (2)
C(36)–C(29)–N(11)	127 (1)	C(31)–C(30)–C(35)	120 (1)	N(10)–C(37)–C(38)	111 (1)	C(39)–C(40)–C(41)	121 (2)
N(10)–C(36)–C(29)	117 (1)	N(11)–C(31)–C(30)	105 (1)	N(10)–C(37)–C(42)	129 (1)	C(40)–C(41)–C(42)	122 (1)
N(10)–C(36)–N(12)	113 (1)	N(11)–C(31)–C(32)	132 (1)	C(38)–C(37)–C(42)	120 (1)	C(37)–C(42)–C(41)	116 (1)
C(29)–C(36)–N(12)	130 (1)	C(30)–C(31)–C(32)	123 (1)				
Perchlorate 1							
Cl(1)–O(1)	1.38 (1)	Cl(1)–O(2)	1.37 (1)	Cl(1)–O(3)	1.376 (9)	Cl(1)–O(4)	1.37 (2)
O(1)–Cl(1)–O(2)	110.9 (9)	O(1)–Cl(1)–O(4)	109 (1)	O(2)–Cl(1)–O(4)	107.3 (9)	O(3)–Cl(1)–O(4)	109.7 (9)
O(1)–Cl(1)–O(3)	112.3 (8)	O(2)–Cl(1)–O(3)	107.5 (8)				
Perchlorate 2							
Cl(2)–O(5)	1.38 (2)	Cl(2)–O(6)	1.40 (1)	Cl(2)–O(7)	1.36 (2)	Cl(2)–O(8)	1.29 (2)
O(5)–Cl(2)–O(6)	107.0 (9)	O(5)–Cl(2)–O(8)	110 (1)	O(6)–Cl(2)–O(8)	108 (1)	O(7)–Cl(2)–O(8)	106 (1)
O(5)–Cl(2)–O(7)	116 (1)	O(6)–Cl(2)–O(7)	110 (2)				

according to Figure 2. Anisotropic temperature factors, hydrogen atom positional parameters, and observed and calculated structure factor amplitudes are given in the supplementary material.

All calculations were performed on a Vax 11/730 DEC computer using the programs SHELX 86,[19] SHELX 76,[18] SDP,[24] and ORTEP[25] and several local subroutines written by J. Aussoleil, F. Dahan, and J. M. Savariault.

Results and Discussion

Synthesis and Compositional Studies. The reaction of ferrous perchlorate with $bimH_2$ or $bbzimH_2$ in methanol under nitrogen atmosphere yields tris chelates as **1** regardless, of the metal to

(24) Frentz, B. A. *SDP-Structure Determination Package*; Enraf-Nonius: Delft, Holland, 1982.

(25) Johnson, C. K. ORTEP. Report ORNL-1794; Oak Ridge National Laboratory: Oak Ridge, TN, 1965.

Table IV. Fractional Atomic Coordinates of Non-Hydrogen Atoms for $[Fe(bbzimH_2)_3]Cl_2 \cdot CH_3OH \cdot 4.33H_2O$ (**2**) with Estimated Standard Deviations in Parentheses

atom	multiplicity	*x/a*	*y/b*	*z/c*
Fe	0.33	0.00000 (0)	0.00000 (0)	0.87382 (6)
N(1)	1.00	0.0905 (7)	0.1340 (6)	0.8413 (2)
N(2)	1.00	0.1415 (6)	0.0789 (6)	0.9027 (2)
N(3)	1.00	0.2437 (7)	0.2590 (7)	0.8308 (3)
N(4)	1.00	0.3024 (7)	0.1945 (8)	0.8990 (3)
C(1)	1.00	0.1830 (8)	0.1844 (7)	0.8519 (3)
C(8)	1.00	0.2098 (8)	0.1540 (8)	0.8840 (3)
C(2)	1.00	0.0877 (8)	0.1818 (8)	0.8107 (3)
C(3)	1.00	0.1846 (9)	0.2585 (8)	0.8036 (3)
C(4)	1.00	0.208 (1)	0.322 (1)	0.7743 (3)
C(5)	1.00	0.128 (1)	0.300 (1)	0.7526 (4)
C(6)	1.00	0.032 (1)	0.224 (1)	0.7594 (3)
C(7)	1.00	0.012 (1)	0.1637 (9)	0.7879 (3)
C(9)	1.00	0.1918 (7)	0.0678 (8)	0.9316 (3)
C(10)	1.00	0.2908 (9)	0.1403 (9)	0.9292 (3)
C(11)	1.00	0.3632 (9)	0.149 (1)	0.9537 (4)
C(12)	1.00	0.327 (1)	0.081 (1)	0.9804 (4)
C(13)	1.00	0.223 (1)	0.0088 (9)	0.9833 (3)
C(14)	1.00	0.1555 (8)	0.0030 (8)	0.9588 (3)
Cl	0.67	0.450 (1)	0.381 (1)	0.8422 (4)
Om(1)	0.33	0.516 (2)	0.396 (2)	0.9091 (8)
C(15)	0.33	0.566 (4)	0.500 (4)	0.899 (1)
Ow(1)	0.33	0.450 (1)	0.381 (1)	0.8422 (4)
Ow(2)	0.11	0.33333 (0)	0.66666 (0)	0.060 (3)
Ow(3)	0.33	0.565 (3)	0.377 (3)	0.789 (1)
Ow(4)	0.33	0.537 (5)	0.436 (5)	1.014 (2)
Ow(5)	0.33	0.527 (4)	0.368 (4)	1.032 (2)

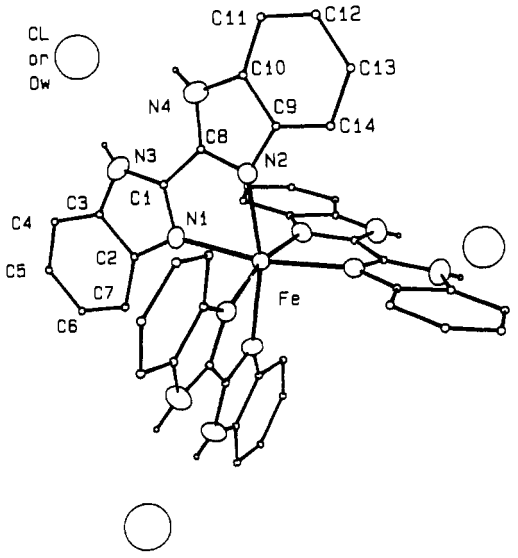

Figure 2. ORTEP view of the $[Fe(bbzimH_2)_3]Cl_2 \cdot CH_3OH \cdot 4.33H_2O$ (**2**) molecule.

ligand stoichiometry. However, when the metal salt includes coordinating anions, i.e. when ferrous chloride is used instead of ferrous perchlorate, tris chelates as **2** or bis chelates as **3** and **4** are synthesized according to the metal to ligand ratio.

The compounds can be obtained without solvate molecule when rapidly precipitated from the reaction mixture or with solvate molecules when slowly crystallized from the same reaction mixture. When the latter conditions are used, **1** crystallizes with one molecule of water, **2** crystallizes with one molecule of methanol and 4.33 molecules of water, and **3** and **4** crystallize with one molecule of methanol.

The reactions of ferrous acetate and ferrous formate with $bimH_2$ and $bbzimH_2$ have been performed only with the 1:2 metal to ligand ratio. No definite complex could be isolated from the reaction of ferrous acetate with $bbzimH_2$. However, the mixture precipitating from the reaction medium seems to contain predominantly the tris chelate $Fe(bbzimH_2)_3(CH_3CO_2)_2$. Complexes **5–7** have been obtained without any solvate molecule regardless of the reaction conditions.

Table V. Selected Interatomic Distances (Å) and Bond Angles (deg) for $[Fe(bbzimH_2)_3]Cl_2 \cdot CH_3OH \cdot 4.33H_2O$ (**2**) with Estimated Standard Deviations in Parentheses

Iron Environment			
Fe–N(1)	2.212 (8)	Fe–N(2)	2.197 (8)
N(1)–Fe–N(1)	91.9 (4)	N(1)–Fe–N(2)	166.5 (4)
N(1)–Fe–N(2)	76.6 (3)	N(2)–Fe–N(2)	97.3 (4)
N(1)–Fe–N(2)	95.5 (4)		
Bibenzimidazole Ligand			
N(1)–C(1)	1.31 (1)	C(2)–C(7)	1.37 (2)
N(1)–C(2)	1.39 (1)	C(4)–C(5)	1.39 (3)
N(2)–C(8)	1.32 (1)	C(5)–C(6)	1.39 (3)
N(2)–C(9)	1.41 (1)	C(6)–C(7)	1.36 (2)
N(3)–C(1)	1.33 (1)	C(9)–C(10)	1.39 (1)
N(3)–C(3)	1.38 (2)	C(9)–C(14)	1.35 (1)
N(4)–C(8)	1.37 (1)	C(10)–C(11)	1.41 (1)
N(4)–C(10)	1.38 (2)	C(11)–C(12)	1.37 (2)
C(1)–C(8)	1.45 (2)	C(13)–C(14)	1.37 (2)
C(2)–C(3)	1.40 (1)		
Fe–N(1)–C(8)	111.1 (7)	C(4)–C(5)–C(6)	123 (1)
Fe–N(2)–C(1)	112.4 (7)	C(5)–C(6)–C(7)	121 (2)
C(1)–N(1)–C(2)	104.9 (8)	C(2)–C(7)–C(6)	119 (2)
C(8)–N(2)–C(9)	106.1 (8)	N(2)–C(8)–C(1)	120.4 (9)
C(1)–N(3)–C(3)	105.4 (9)	N(2)–C(8)–N(4)	113 (2)
C(8)–N(4)–C(10)	106.2 (8)	N(4)–C(8)–C(1)	127.5 (9)
N(1)–C(1)–N(3)	115 (2)	N(2)–C(9)–C(10)	107.9 (9)
N(1)–C(1)–C(8)	118.3 (8)	N(2)–C(9)–C(14)	129.6 (9)
N(3)–C(1)–C(8)	127 (1)	C(10)–C(9)–C(14)	122 (2)
N(1)–C(2)–C(3)	108 (2)	N(4)–C(10)–C(9)	108 (2)
N(1)–C(2)–C(7)	131.9 (9)	N(4)–C(10)–C(11)	129 (1)
C(3)–C(2)–C(7)	120 (2)	C(9)–C(10)–C(11)	123 (2)
N(3)–C(3)–C(2)	106.9 (9)	C(10)–C(11)–C(12)	115 (2)
N(3)–C(3)–C(4)	130 (2)	C(11)–C(12)–C(13)	122 (1)
C(2)–C(3)–C(4)	123 (1)	C(12)–C(13)–C(14)	122 (1)
C(3)–C(4)–C(5)	114 (1)	C(9)–C(14)–C(13)	116.7 (9)
Methanol Molecule			
Om(1)–C(15)	1.44 (6)		

The $bimH_2$ and $bbzimH_2$ ligands are involved in their fully protonated form in this series of complexes, and the analytical results indicate the presence of two perchlorate, chloride, or carboxylate counterions in complexes **1–7**. When isolated as solids, complexes **1** and **2** are not oxidized on exposure to the air, even for days. On the contrary, **3–7** are very rapidly oxidized on exposure to the aerial oxygen.

Molecular Structure of 1. The structure consists of mononuclear cations, $[Fe(bbzimH_2)_3]^{2+}$, separated by ClO_4 anions, and molecules of water of crystallization, as shown in Figure 1. The cation comprises a central iron atom coordinated to three bidendate $bbzimH_2$ ligands, referred to as L_1, L_2, and L_3, affording an FeN_6 distorted coordination octahedron, as evidenced by the range of iron–nitrogen distances (2.12 (2)–2.22 (2) Å and N–Fe–N angles (76.3 (3)–99.8 (4)°) (Table III). This distortion is also evidenced by the range of dihedral angles between the N–Fe–N planes corresponding to the L_1 to L_3 ligands (94.9 (2)–100.2 (2)°).[15]

Each benzimidazole unit of L_1, L_2, L_3 is planar, the deviations of the non-hydrogen atoms of each unit from their mean plane being less than 0.05 Å. However, the two benzimidazole moieties of each $bbzimH_2$ ligand are not coplanar, their dihedral angles being equal to 166 (2), 173 (2), and 172 (2)° for L_1, L_2, and L_3, respectively.[15] Similar observations have been previously reported for metal complexes including biimidazole or biimidazolate ligands.[10,26-28] As previously observed by Mighell et al.,[26] the exterior angles (N(1)–C(1)–C(8) and N(3)–C(1)–C(8) for example) are modified by coordination. The short C–C single bond that con-

(26) Mighell, A. D.; Reimann, C. W.; Mauer, F. A. *Acta Crystallogr., Sect. B: Struct. Crystallogr. Cryst. Chem.* **1969**, *25*, 60–66.
(27) Kaiser, S. W.; Saillant, R. B.; Butler, W. M.; Rasmussen, P. G. *Inorg. Chem.* **1976**, *15*, 2688–2694.
(28) Uson, R.; Gro, L. A.; Gimeno, J.; Ciriano, M. A.; Cabeza, J. A.; Tiripicchio, A.; Tiripicchio Camellini, M. *J. Chem. Soc., Dalton. Trans.* **1983**, 323–330.

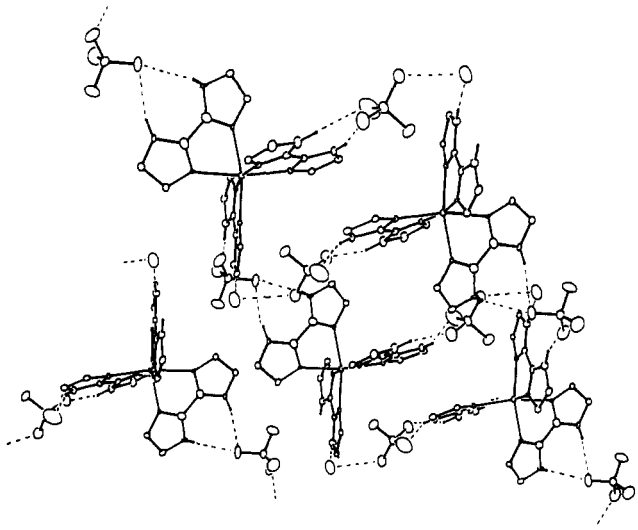

Figure 3. Projection of five $[Fe(bbzimH_2)_3](ClO_4)_2 \cdot H_2O$ molecules onto the [010] plane showing the hydrogen bond network (dotted lines). For clarity, the benzene rings of the $bbzimH_2$ ligands have been omitted.

nects the two benzimidazole units, the near coplanarity of these units, and the relatively narrow range of observed bond distances indicate the importance of resonance in the bonding description of the L_1 to L_3 $bbzimH_2$ ligands.

The bond lengths and angles of the perchlorate anion containing Cl(1) are in the usual ranges. On the contrary, the perchlorate anion containing Cl(2) exhibits an unusually large range of bond lengths (1.29–1.40 Å) and angles (106–116°). The large values of the thermal parameters of the oxygen atoms O(7) and O(8)[15] imply a large O(7)–Cl(2)–O(8) deformation vibration resulting in the spreading of the electronic density over a banana-like volume. Fitting such a volume to a sphere (or an ellipsoid) results in an apparent shortening of the bond length.[29] The correction suggested by Cruickshank[30] affords bond length values similar to those usually observed for perchlorate anions, i.e. Cl(2)–O(7) = 1.38 (2) Å and Cl(2)–O(8) = 1.39 (2) Å.

Each N–H group of the asymmetric unit is hydrogen-bonded to perchlorate or water oxygen atoms. The resulting hydrogen-bond network affords infinite sheets along [010], as illustrated in Figure 3. The corresponding interatomic distances and angles are listed in the supplementary material. The infinite sheets are packed along [010] through benzene ring stackings to afford the resulting crystal structure. A view of the unit cell along [001] is included in the supplementary material.

Molecular Structure of 2. The unit cell is hexagonal and results from the compact packing of the nearly spheric $[Fe(bbzimH_2)_3]^{2+}$ cations. The chloride anions and methanol and water molecules are situated in the interstices and provide the cohesion of the cations through a hydrogen-bond network involving all the N–H groups and chlorine and oxygen atoms. The interatomic distances and angles corresponding to these hydrogen bonds are listed in the supplementary material.

The two chloride anions and one water molecule are statistically disordered over three sites, as illustrated in Figure 2. This allows axial symmetry involving a C_3 crystallographic axis. The iron atom is located on this ternary crystallographic axis, and the three $bbzimH_2$ ligands are arranged like the blades of a screw propeller. The six Fe–N bond distances are almost identical, and the distortion from the pure octahedral geometry results from the narrow N(1)–Fe–N(2) angle (76.6 (3)°) imposed by the bibenzimidazole bite (Table V). The resulting distortion can be described as a compression along the [1,1,1] trigonal axis of the octahedron.

Each $bbzimH_2$ ligand experiences a conformation similar to that previously described in the case of complex **1**. The deviations of the non-hydrogen atoms of each benzimidazole unit from their mean plane and the dihedral angle between the two mean planes of the $bbzimH_2$ ligand are listed in the supplementary material.

Comparison of the Molecular Structures of 1 and 2. In both complexes, three $bbzimH_2$ groups act as bidentate ligands through the lone pairs of the imine nitrogen atoms of their imidazole rings. Consequently, each ligand imposes a small N–N bite resulting in a narrow N–Fe–N angle (~77°) and a distorted-octahedral ligand environment for the ferrous ion.

In the case of complex **2**, the iron(II) atom is located on a ternary crystallographic axis and the ligand environment may be described as a trigonal antiprism. In the case of complex **1**, a ligand environment similar to that of complex **2** is observed although the iron is not located on a C_3 crystallographic axis. Each $bbzimH_2$ ligand is characterized by a different interaction network with either a perchlorate anion or a water molecule, resulting in different iron–nitrogen bond distances and angles. The nitrogen atoms corresponding to the three largest Fe–N bonds (N(1), N(2), N(5)) are located at the apices of one face of the octahedron, and those corresponding to the three shortest Fe–N bonds are situated at the apices of the opposite face. Consequently, the ligand environment of complex **1** can be described as a rhombically distorted octahedron.

Structural Hypothesis for Complexes 3–7. Taking into account the absence of solvate molecules in the formulation of complexes **5–7** and the fact that complexes **3** and **4** can be prepared either with or without a methanol molecule, it can be considered that the coordination sphere of these five complexes includes two bidentate $bimH_2$ or $bbzimH_2$ ligands and two chloride or carboxylate anions. Furthermore, the variation of the magnetic moment of **3–7** with temperature in the 300–4 K range is not large enough to suggest extented magnetic interactions corresponding to polymeric or chain structures for these complexes (see magnetic susceptibility section). Thus, the only structural arrangements that we shall consider in order to distribute the two bidentate $bimH_2$ or $bbzimH_2$ ligands and the two chloride or carboxylate anions among the six coordination positions of the ferrous ion are the cis and trans arrangements.

Actually, both structural arrangements have been already evidenced for the coordination of $bimH_2$ to transition-metal ions.[10,26] However, McKenzie[31] has shown that a trans arrangement results in a steric hindrance between the α-hydrogen atoms pertaining to the rings of the trans 2,2'-bipyridine or 1,10-phenanthroline L ligands of $[ML_2X_2]$ chelates. Molecular models evidence that the steric hindrance is even larger when 2,2'-bipyridine or 1,10-phenanthroline chelating ligands are replaced by 2,2'-bibenzimidazole in a $[ML_2X_2]$ chelate.

These observations imply that the cis structural arrangement is highly favored compared to the trans arrangement in the bis chelates including $bbzimH_2$, i.e. **4** and **7**. Concerning complexes **3**, **5**, and **6**, which include two $bimH_2$ ligands, examination of molecular models indicates that the cis isomer is also favored; however, in that case the trans structural arrangement cannot be discarded.

IR Spectroscopy. Table VI lists some pertinent IR frequencies for the isolated ligands and their iron(II) complexes together with our proposed assignments. The overall appearance of the spectra of the complexes is similar to that of the isolated ligands and includes the following general features. The NH + CH stretches are observable as very broad absorptions spread out from ca. 3200 to 2400 cm^{-1}. The N–H in-plane bending frequencies are observed near 1580 and 1150 cm^{-1}. The benzene and imidazole ring stretching absorptions are observable in the 1500–1400-cm^{-1} range, while a characteristic imidazole ring stretching frequency is observed around 1330 cm^{-1}. The C–H in-plane bending frequencies are in the 950–900-cm^{-1} range. The imidazole rings are characterized by in-plane ring bendings, affording two to three absorptions located between 780 and 750 cm^{-1}, and ring torsions, affording two absorptions observable in the 690–610-cm^{-1} range. The $bbzimH_2$ ligands afford a benzene out-of-plane bending ab-

(29) Willis, B. T. M.; Pryor, A. W. *Thermal Vibrations in Crystallography*; Cambridge University Press, Cambridge, England, 1975; pp 199–200.
(30) Cruickshank, D. J. W. *Acta Crystallogr., Sect. B: Struct. Crystallogr. Cryst. Chem.* **1956**, *9*, 757.
(31) McKenzie, E. D. *Coord. Chem. Rev.* **1971**, *6*, 187–216.

Table VI. Significant IR Absorptions (cm^{-1}) of $bimH_2$, $bbzimH_2$, and Complexes 1–7

	$bimH_2$	$bbzimH_2$	1	2	3	4	5	6	7
ν_{N-H}	3173–2544	3133–2443	3196–2520	3140–2520	3189–2413	3133–2520	3130–2459	3115–2462	3163–2650
ν_{N-H} (in-plane bend)	1580 s, 1543 m	1586 s	1589 m	1587 m	1523 s	1586 s	1571 s	1584 s	1585 s
ring str	1433 m, 1403 s	1497–1396	1501–1419	1500–1399	1499 m, 1419 s	1498–1418	1459–1380	1438 m, 1425 m	1477–1399
imidazole ring str	1333 s	1343 s	1350 s	1349 s	1312 s	1349 s	1316 s	1306 s	1347 s
ν_{N-H} (in-plane bend)	1144 m	1143 ms	1149 s	1145 m	1172 m	1146 m	1180 m	1181 mw	1146 m
ν_{C-H} (in-plane bend)	939 s, 915 m	948–900	953–903	949–900	936 m, 921 w	957–900	949–917	939 m, sh	972–886
imidazole in-plane ring bend	763 ms, 748 s, 736 m	777 mw, 765 mw	777 m, 765 m	777 s, 765 s	782 m, 758 s	777 m, 765 s	779 m, 754 s	758 s, 746 s	777 m, 755 m
benzene out-of-plane bend		743 s	746 s	738 s		740 s			742 s
imidazole ring torsion	689 s, 616 w	662 m, 618 w	652 m, 606 m	655 m, 606 m	686 s, 624 m	654 m, 606 m	646 m, 617 w	693 s, 628 w	639 w, 607 w
benzene ring torsion		587–428	581–429	582–430		582–430			583–431
ν_{Fe-L}			461 w, 280 m	457 w, 280 m	490 m, 427 m, 273 m, 200 m	460 sh, 279 w	513 m, 467 m, 429 m, 353 w, 302 w, 258 ms	462 mb, 426 m, 375 w, 280 mb	466 w, 320 m, 282 m, 260 m
ν_{OH} (solvate)			3323 s	3300 sh	3400 sh	3400 sh			
ν_{COO^-} ν(as)							1602 s	1593 s	1592 s
ν_{COO^-} ν(s)							1410 s	1306 s	1390 s
ν_{C-H} (CH_3OH bend)					1389 m	1381 m			
ν_{C-O} (CH_3OH str)					1261 m	1255 w			
$\nu_{ClO_4^-}$ ν_4			1139 s, 1099 s						
$\nu_{ClO_4^-}$ ν_3			630 m, sh, 624 ms						

Table VII. Summary of Magnetic Susceptibility Data (μ_B/Fe (μ_B)) for Complexes 1–7[a]

		T, K				
no.	complex	300	100	45	25	5
1	$[Fe(bbzimH_2)_3](ClO_4)_2$	5.24	5.27	5.25	5.27	4.77
2	$[Fe(bbzimH_2)_3]Cl_2$	5.28	5.35	5.08	4.90	3.91
3	$Fe(bimH_2)_2Cl_2$	5.27	5.27	5.13	5.20	5.43
3*		(5.07)	(5.02)	(4.92)	(5.00)	(4.26)
4	$Fe(bbzimH_2)_2Cl_2$	5.28	5.22	5.16	5.06	4.11
5	$Fe(bimH_2)_2(CH_3COO)_2$	5.48	5.42	5.15	4.78	4.40
6	$Fe(bimH_2)_2(HCOO)_2$	5.38	5.35	5.23	5.17	4.82
7	$Fe(bbzimH_2)_2(HCOO)_2$	5.47	5.50	5.24	5.00	3.96

[a] Samples were obtained by packing the microcrystalline materials in the sample holder, with the exception of sample 3* being in the form of a Vaseline mull.

sorption near 740 cm^{-1} and three to four benzene ring torsion frequencies located bwteen 587 and 428 cm^{-1}.

As evidenced by the presence of the N–H stretching and bending absorptions in all seven complexes and the crystal molecular structure of **1** and **2**, the $bimH_2$ and $bbzimH_2$ ligands are coordinated to the metal center of compounds **1**–**7** in their fully protonated form. This is also confirmed by the presence of two perchlorate or chloride or carboxylate counterions in the formulation of the studied complexes.

The involvement of the imine nitrogen atoms of the imidazole rings in the coordination to the metal center in a bidentate mode is evidenced not only by the crystal molecular structure of **1** and **2** but also by the fact that the imidazole in-plane ring bending and ring torsion absorptions experience larger shifts in complexes **3**, **5**, and **6**, including $bimH_2$, than in complexes **1**, **2**, **4**, and **7**, including $bbzimH_2$, comparatively to the isolated ligands. This observation is in agreement with the fact that in-plane ring bendings and ring torsions are already restricted by the fusion of the imidazole moiety to the benzene ring in the uncoordinated $bbzimH_2$ ligand. Consequently, the coordination of both imine nitrogen atoms of $bbzimH_2$ should not further reduce these motions. On the contrary, the involvement of the same atoms of $bimH_2$ in the coordination to a metal center should significantly restrict these ring motions.

The absorption frequencies of uncoordinated $bimH_2$ and $bbzimH_2$ listed in Table VI evidence that $bimH_2$ has no vibrational bands in the 600–200-cm^{-1} range while $bbzimH_2$ has four characteristic benzene ring torsion absorptions in this range. Consequently, it may be assumed that absorptions occurring in the 600–200-cm^{-1} range for the seven complexes are an effect of coordination with the exception of the four characteristic benzene ring torsion frequencies observed in complexes **1**, **2**, **4**, and **7** between 587 and 428 cm^{-1}. Among these low-frequency vibrational bands, it may be assumed, in accordance with previous IR and Raman spectroscopic studies,[32,33] that the absorption observed between 280 and 258 cm^{-1} for the seven complexes is a N–M–N bending frequency.

As usually observed, the ν_3 and ν_4 modes of the ClO_4^- anion occur at ca. 1100 and 620 cm^{-1}, respectively, for complex **1**. The splitting of both absorptions indicates a reduction in the T_d symmetry of the free ion.[34] In view of the X-ray crystal structure determination of **1**, we attribute this splitting to hydrogen-bonding interactions with the N–H groups of the ligands.

The presence of a methanol solvate molecule, assumed for complexes **3** and **4** on the grounds of the elemental analyses, is further confirmed by the observation of the characteristic OH stretching, CH_3 bending, and C–O stretching modes near 3400, 1385, and 1260 cm^{-1}, respectively.

Finally, the asymmetric and symmetric COO^- absorptions are observed for **5**–**7** in the usual 1590- and 1400-cm^{-1} regions, respectively.

(32) Cordes, M. M.; Walter, J. L. *Spectrochim. Acta* **1968**, *24A*, 1421–1435.
(33) Goodgame, B. M. L.; Goodgame, M.; Rayner Canham, G. W. *Inorg. Chim. Acta* **1969**, *3*, 406–410.
(34) Burnett, M. G.; McKee, V.; Nelson, S. M. *J. Chem. Soc., Dalton. Trans.* **1981**, 1492–1497.

Table VIII. Summary of Mössbauer Parameters (mm s^{-1}) for Complexes **1–7**

		300 K		83 K		4.2 K	
no.	complex	δ	ΔE_Q	δ	ΔE_Q	δ	ΔE_Q
1	$[Fe(bbzimH_2)_3](ClO_4)_2$	1.03	0.90	1.14	1.59	1.16	1.77
2	$[Fe(bbzimH_2)_3]Cl_2$	1.08	2.50	1.18	3.12	1.21	3.05
3	$Fe(bimH_2)_2Cl_2$	1.05	3.85	1.18	4.02	1.18	3.96
4	$Fe(bbzimH_2)_2Cl_2$	1.08	2.65	1.20	3.20	1.22	3.16
5	$Fe(bimH_2)_2(CH_3COO)_2$	1.1	1.6	1.2	1.9	1.2	2.0
				1.2	2.4	1.2	2.4
6	$Fe(bimH_2)_2(HCOO)_2$	1.10	3.73	1.21	3.81	1.23	3.75
7	$Fe(bbzimH_2)_2(HCOO)_2$	1.02	3.03	1.13	3.14	1.16	3.15

	200 K		4.2 K	
	δ	ΔE_Q	δ	ΔE_Q
bacterial reaction centers[a]	1.11	1.84	1.18	2.22
PS2 particles[b]	1.13	2.23	1.18	2.65

[a] From ref 40. [b] From ref 3c.

Magnetic Susceptibility. The molar magnetic moments of powdered samples of complexes **1–7** determined in the 300–4.2 K temperature range are gathered in Table VII. The effective magnetic moment per iron at 300 K is generally higher than the spin-only value of 4.9 μ_B for $S = 2$, as usually observed for high-spin iron(II) complexes. It is notable that the magnetic moment of the iron(II) in bacterial reaction centers is also high, 5.35 μ_B/Fe.[35] The relatively small dependence of the magnetic moment on temperature indicates that none of these complexes experiences magnetic exchange interactions. This conclusion agrees well with the results of the X-ray structural determination showing that the shortest Fe–Fe distances are 9.47 and 9.09 Å in **1** and **2**, respectively. It also suggests the absence of bridging ligands in complexes **3–7**.

The decrease in the magnetic moment of complexes **1**, **2**, and **4–7** is mainly situated between 25 and 4.2 K, indicating the presence of moderate zero-field splitting of the high-spin iron(II) ground state. The results in Table VII agree with the Mössbauer data, and for some complexes the data are similar to those of the bacterial iron(II).[35]

The μ_B/Fe values obtained from polycrystalline samples of **3** show that the magnetic moment increases to 5.43 μ_B/Fe at 5 K. This magnetic behavior is thought to arise from alignment of the crystallites in the magnetic field.[36] In order to assess the origin of this behavior, the magnetic susceptibility of **3** was also measured on a Vaseline mull of the sample. The resulting values (Table VII, figures with parentheses) show a slight lowering of μ_{eff} at all temperatures, such that μ_B/Fe remains approximately constant down to 25 K, below which it decreases to 4.26 μ_B/Fe. These results confirm the interpretation of the values obtained for the polycrystalline samples of **3** and are in agreement with the behavior expected for a high-spin iron(II) complex in which there is zero-field splitting of the ground state.

Mössbauer Spectroscopy. The Mössbauer spectra of complexes **1–4**, **6**, and **7** recorded at 300, 83, and 4 K consist of a single quadrupole-split doublet. The spectra of **5** consist of two overlapping quadrupole-split doublets. The spectra were least-squares-fitted with Lorentzian lines. The resulting isomer shift (δ) and quadrupole-splitting parameters (ΔE_Q) are listed in Table VIII, and the corresponding least-squares-fitted spectra are deposited as supplementary material. The δ and ΔE_Q values clearly indicate the presence of high-spin iron(II) in all complexes. The δ values are weakly temperature dependent due to second-order Doppler shift.[37] With the exception of **1** and possibly one of the two components in **5**, the low-temperature ΔE_Q values are relatively large, indicating that the T_{2g} orbital triplet is split by crystal field distortions, affording lower than octahedral symmetry, and that the lower state is an orbital singlet. Decrease of ΔE_Q at room temperature indicates the presence of excited T_{2g} levels within thermal reach in some of the complexes (**1**, **2**, **4**, **5**).[38]

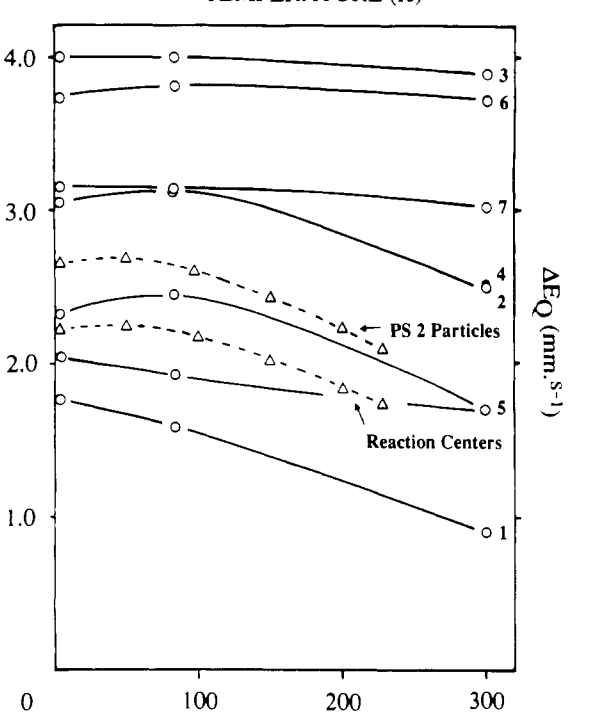

Figure 4. Variation of the quadrupole splitting for complexes **1–7**, PS 2 particles, and bacterial reaction centers with temperature. The solid lines drawn between the experimental values of complexes **1–7** are intended to connect the values corresponding to a given complex and do not represent calculated values.

A qualitative examination of the Mössbauer data can provide useful information concerning the nature and extent of the distortion from the regular octahedral symmetry for each complex. The crystal and molecular structure of $[Fe(bbzimH_2)_3]Cl_2$ (**2**) indicates that the distortion of the octahedral geometry is essentially axial and results from a compression along C_3. Consequently, the ground state must be the $|z^2\rangle$ orbital singlet. The 3.05 mm s^{-1} ΔE_Q value at 4.2 K is in agreement with a singlet ground state, and the 2.5–3.12 mm s^{-1} ΔE_Q variation in the 300–80 K temperature range indicates that the energy separation between the singlet ground state and the higher orbital states is small enough to allow thermal population of the higher orbital states at 300 K. The low-temperature maximum ΔE_Q value is about 20% lower than the maximum value of 4 mm s^{-1} expected for an isolated singlet ground state.[39] This can be attributed to the effect of the spin–orbit interaction. An axial splitting, Δ, 5–6 times greater than the spin–orbit constant, λ, would qualitatively explain both the temperature dependence of ΔE_Q and the reduced low-temperature maximum.[38] Similar comments can be made for complex **4**, for which crystallographic data are not available. The somewhat weaker temperature dependence and larger ΔE_Q values support a somewhat higher Δ/λ ratio for the latter.

In the case of $[Fe(bbzimH_2)_3](ClO_4)_2$ (**1**), the crystal structure indicates a rhombic distortion of the octahedral geometry including an axial compression along a pseudotrigonal axis; consequently, with a $|z^2\rangle$ singlet ground state, the rhombic distortion will split the higher doublet into two higher orbital states. The 1.77 mm s^{-1} ΔE_Q value at 4.2 K and the strong temperature dependence indicate that the energy separation between the ground state and the first higher orbital state is small enough to result in a significant thermal population of the latter even at liquid-helium temperature. For such small orbital level separations, the role of the spin–orbit coupling becomes very important and an understanding of the

(35) Butler, W. F.; Johnston, D. C.; Okamura, M. Y.; Shore, H. B.; Feher, G. *Biophys. J.* **1980**, *32*, 967–992.
(36) Kennedy, B. J.; Murray, K. S. *Inorg. Chem.* **1985**, *24*, 1552–1557 and references therein.
(37) Greenwood, N. N.; Gibbs, T. C. *Mössbauer Spectroscopy*; Chapman and Hall: New York, 1971; Chapter 6.
(38) Ingalls, R. *Phys. Rev.* [Sect. A] **1964**, *133*, 787–795.
(39) Sams, J. R.; Tsin, T. B. *Inorg. Chem.* **1975**, *14*, 1573–1579.

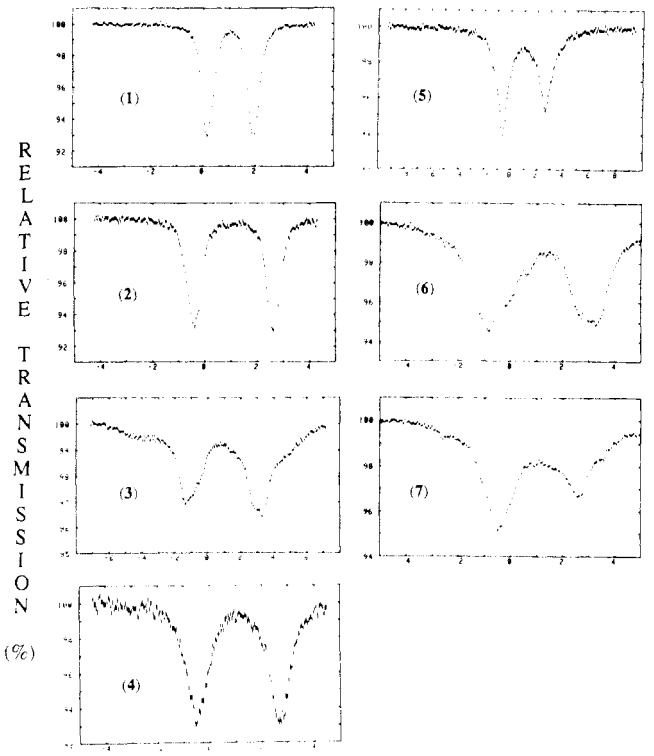

Figure 5. 4.2 K Mössbauer spectra of **1–7** in an applied magnetic field of 9 kOe.

system would require much more elaborate studies, which are beyond the scope of this paper.

Complexes **3** and **6** exhibit a ΔE_Q value of ca. 4 mm s^{-1}, which is practically independent of the temperature in the 300–4 K range. Such large and temperature-independent quadrupole splittings imply that the ground state is an orbital singlet and that the energy separation between the ground state and the higher orbital states is very large, i.e. that the crystal field distortion of the octahedral symmetry has a strong axial term. A comparison with the diagrams in ref 38 indicates that for these complexes $\Delta/\lambda > 10$. Although its ΔE_Q values are significantly smaller, complex **7** has a very weak temperature dependence of ΔE_Q in similarity with **3** and **6**. A possible explanation is that crystal field splittings are also large for this complex but covalency effects have reduced the ΔE_Q values. The latter assumption is also supported by the smaller isomer shift values for this complex.

Finally, it is difficult to draw any simple conclusions for complex **5**, which is characterized by two components, both in the range of ΔE_Q requiring a multiparameter approach in the analysis.

Additional information about the crystal field distortions in the various complexes can be obtained by the study of the spectra in an applied magnetic field. Representative spectra at 4.2 K in a field of ca. 9 kOe are shown in Figure 5. Although a detailed analysis of these spectra is beyond the scope of this study, it may be noted that they qualitatively support the above conclusions of the quadrupole-splitting interpretation. The zero-field splitting of the ground-state spin quintet, parameter D in the spin Hamiltonian formalism, is to a first approximation inversely proportional to the axial field splitting, Δ, of the T_{2g} levels. For large Δ, D is small and an applied magnetic field will be more efficient in producing a magnetic splitting of the Mössbauer spectra via mixing of the spin quintet levels. This trend is indeed observed in the spectra of Figure 5 where compounds **3**, **6**, and **7**, characterized by the smallest temperature variation of the quadrupole splitting (therefore the larger Δ), show the largest splitting in an applied magnetic field.

The above qualitative considerations are also valid in the case of rhombic distortions and even in the unlikely possibility of relaxation effects. The latter would alter significantly the interpretation of the spectra only in the case of a negative axially symmetric zero-field splitting. On the basis of the low ΔE_Q values, the only compound that could have a doublet ground state is **1**; this complex however shows the smallest splitting in the presence of an applied magnetic field.

In Table VIII and Figure 4 the Mössbauer parameters of complexes **1–7** are compared to those of the iron(II)–quinone complex of the *Rhodobacter sphaeroides* R-26 reaction centers[40] and of PS 2 particles from *Chlamydomonas reinhardtii*.[3c] In the bacterial reaction centers, the iron is in a highly distorted octahedral environment composed of four imidazole nitrogens and a glutamic acid residue possibly acting as a bidentate ligand.[4,5] The iron(II) in photosystem 2 is also believed to have the four imidazole ligands, but the identity of the axial ligand(s) is less definitive. Mössbauer studies of photosystem 2 preparations from spinach[3e] show at least two components with quadrupole splittings ranging from 2.1 to 2.9 mm s^{-1} at 77 K and with temperature variation parallel to that observed in the PS 2 particles in Figure 4. The isomer shift values are in all cases compatible with octahedral geometry and nitrogen and oxygen ligands. Recent studies[41] show that ligand replacement is possible in the PS 2 iron and HCO_3^-/CO_2 is the most likely axial ligand under physiological pH.

The iron centers in **4** and **7** are coordinated to two $bbzimH_2$ ligands, which are necessarily cis to each other for steric reasons, and two chloride or formate anions, respectively. The large increase in ΔE_Q values from **4** and **7** to **3** and **6** cannot be explained by the replacement of $bbzimH_2$ (**4** and **7**) by $bimH_2$ (**3** and **6**). As the steric requirement for a cis arrangement is not as strong in **3** and **6** as in **4** and **7**, the substantial increase in the ΔE_Q values indicates a trans arrangement in the former complexes. Although this interpretaton is in agreement with the general trend of the trans complexes having higher ΔE_Q values than the cis complexes,[37] it should be noted that in high-spin iron(II) complexes the dominant contribution to the quadrupole splitting comes from the 3d electrons and is not therefore a direct reflection of the electric field gradient of the ligands.

The presence of both cis and trans isomers may also explain the observation of two components in the spectra of complex **5**. Interestingly enough, this complex, which has a $(bimH_2)_2$-$(CH_3CO_2)_2$ ligand environment, shows the closest analogy of ΔE_Q and δ values to the bacterial iron(II) complex.

The relatively large variation in the Mössbauer properties among this set of rather similar complexes indicates that in addition to the nature of the ligands the distortion of the Fe(II) coordination sphere is a factor that has to be taken into account in designing proper spectroscopic analogues of the photosynthetic mononuclear non-heme ferrous complexes.

Acknowledgment. We thank the Etablissement Public Régional and the CNRS (Action de Recherche Intégrée "Chimie Biologie" and ATP Photosynthèse) for partial support of this work. The Greek Ministry of Research and Technology and the French Ministère des Affaires Etrangères are gratefully acknowledged for partial support of this work through the Greek-French Scientific Exchange Program.

Supplementary Material Available: Figures 6 and 7, showing a view of the unit cell of complex **1** along [001] and the least-squares-fitted Mössbauer spectra of complexes **1–7**, respectively, Table IX, listing the analytical results for complexes **1–7**, and Tables X–XIX, listing crystallographic data, hydrogen atom positional parameters, final non-hydrogen atom thermal parameters, dihedral angles between N–Fe–N planes, interatomic distances and bond angles for the hydrogen-bonded atoms, and deviations of atoms from least-squares planes of the benzimidazole moieties of a bibenzimidazole ligand and dihedral angles between these planes for complexes **1** and **2**, respectively (15 pages); Tables XX and XXI, listing the observed and calculated structure factor amplitudes for complexes **1** and **2**, respectively (22 pages). Ordering information is given on any current masthead page.

(40) Boso, B.; Debrunner, P.; Okamura, M. Y.; Feher, G. *Biochim. Biophys. Acta* **1981**, *638*, 173–177.
(41) (a) Petrouleas, V.; Diner, B. A. *Biochim. Biophys. Acta* **1990**, *1015*, 131–140. (b) Diner, B. A.; Petrouleas, V. *Biochim. Biophys. Acta* **1990**, *1015*, 141–149.